CrossMark

ORIGINAL PAPER

# Vipulanandan Models to Predict the Mechanical Properties, Fracture Toughness, Pulse Velocity and Ultimate Shear Strength of Shale Rocks

**Ahmed S. Mohammed**

**Abstract** This study was focused on investigating the correlations between the physical and mechanical properties and geostatistical analysis of the shale rock based on the experimental data and the data collected from various research studies. In this study, over 250 data were used to characterize the shale rock behavior. The compressive strength and tensile strength of the shale rock investigated varied up to 200 and 13 MPa respectively. The shale rock was characterized based on the density, modulus of elasticity, fracture toughness and tensile strength and correlating the properties to compression strength and pulse velocity. Based on the statically analysis, the density of shale was in the range of 1.70–2.78 gm/cm$^3$. Vipulanandan correlation model was effective in relating the modulus of elasticity, pulse velocity, fracture toughness with the compressive strength of the rocks. There was no direct correlation between the compressive strength and density or tensile strength and density of the shale rock. The new Vipulanandan failure model has been used to not only better quantify the tensile strength but also to predict the maximum shear stress of the rock. The prediction of the Vipulanandan failure model for shale rock type was also compared to the Mohr–Coulomb failure model. The Vipulanandan failure model has a maximum shear stress limit were, as the Mohr–Coulomb failure model did not have a limit on the maximum shear stress. Based on the Vipulanandan failure model the maximum shear stresses produced by the shale was 103 MPa. Based on the coefficient of determination ($R^2$) and the root mean square error values, the Vipulanandan failure model predicted the results better than the Mohr–Coulomb model.

**Keywords** Shale rock · Physical properties · Failure model criteria · Nondestructive test · Statistical analysis · Modeling

## 1 Introduction

Shale oil is unconventional oil, which is produced from oil shale pyrolysis, hydrogenation, or thermal dissolution. Generally, the term oil shale is given to any type of sedimentary rock that contains solid bituminous materials (called kerogen) that are released from petroleum like liquids when the rock is heated in the chemical process of pyrolysis (Sandrea 2012). Formation of oil shale was from the same process as that in which the crude oils were generated millions of years ago mainly by deposition of organic debris on ocean, lake, and sea beds. The oil shale is sometimes called "the rock that burns" as it contains enough oil to burn itself (Omar 2017). In the United States shale gas and oil production has grown rapidly

A. S. Mohammed (✉)
Department of Engineering, The American University of Iraq, Sulaimani-Iraq, Kurdistan Region, Sulaymaniyah, Iraq
e-mail: ahmed.salih@auis.edu.krd

in the past years with continuous technological developments in hydraulic fracturing. Hydraulically fracturing rocks increases the permeability by opening, connecting and keeping open pre-existing or new fractures in the formation (Vipulanandan et al. 2015a). For tunneling through the rocks to place, the necessary infrastructure there is a need for better quantification of the mechanical properties and failure criteria for the shale rock. The design of drilled foundations, footings, and rafts in shale rock requires quantification of the strength properties of the rock in order to be rational; most problems in rocks during construction and hydraulic fracturing require the tensile strength, modulus, fracture toughness and failure model for the in situ rock. Based on this study, using only the unconfined compression strength of the rock (normally very limited number of samples are available for testing), the tensile strength and compression modulus can be determined (Swapnil et al. 2004). Since the sampling of these materials is difficult and costly, it is important to characterize shale rocks with minimum testing. Nondestructive tests are increasingly being used in rapidly evaluating the properties of construction materials. The nondestructive evaluation of rock properties is useful for preliminary prediction of static properties. The vibration method and the ultrasonic pulse velocity method are some of the most commonly used nondestructive testing methods for construction materials (Swapnil et al. 2004). The pulse velocity method has the advantage that, generally, it does not depend on the size or the shape of the specimen and can be applied well to construction materials. At present, Mohr–Coulomb criteria is used to characterize the failure of the rocks, but it does not quantify the tensile strength and has no limit on the maximum shear strength tolerance for rocks. In addition, there is very limited property correlation in the literature for the shale rock. Hence, there is a need for developing improved failure criteria and property correlations for the rocks (Swapnil et al. 2004; Omar 2017).

Uniaxial compressive strength (UCS), the most widely used parameter to evaluate rock strength, requires expensive and time-consuming testing with sample preparation (Karakus et al. 2005). Many researchers have tried to predict UCS based on simpler, faster, and less expensive physical tests by means of statistical methods. For this purpose, researchers have introduced several empirical equations for determination of rock strength via simple

physical properties. By means of such properties, rock strength may be determined in an easy, quick, and inexpensive manner during field investigations (Sabatakakis et al. 2008; Rajabzadeh et al. 2012). In geotechnical and rock engineering, most applied rock classification systems are based on mechanical parameters such as uniaxial compressive strength (UCS), tensile strength ($\sigma_t$) and Young's modulus or deformability modulus (E). Tensile strength and fracture toughness are an important parameter in rock mechanics, and is amongst other things used as a criterion for initiation and propagation of fractures in hydraulic fracture modeling (Meng and Pan 2007; Vipulanandan and Mohammed 2015a). The unconfined compressive strength (UCS) and angle of internal friction ($\phi$) of sedimentary rocks are key parameters needed to address a range of geomechanical problems ranging from limiting wellbore instabilities during drilling (Moos et al. 2003), to assessing sanding potential and quantitatively constraining stress magnitudes using observations of wellbore failure (Zoback et al. 2003).

## 1.1 Vipulanandan Correlation Model

The Vipulanandan hyperbolic model has been used to present the behavior of cement and polymer modification soils (Usluogullari and Vipulanandan 2011). Mohammed and Vipulanandan (2014, 2015) used the Vipulanandan hyperbolic relationship to predict the relation between the compressive and tensile strength of sulfate contaminated CL soils. Vipulanandan and Mohammed (2014) used the Vipulanandan hyperbolic relationship to predict the maximum shear stress limit for the bentonite drilling mud modified with the polymer. The Vipulanandan hyperbolic model was used to predict the rheological properties with the electrical resistivity of nanoclay modified bentonite-drilling muds (Vipulanandan and Mohammed 2015b). For shear thinning fluids, the shear stress-shear strain rate relationship is nonlinear with a limit of the maximum shear stress tolerance. Similar trends has been observed in many other engineering and environmental applications and has been modelled using the Vipulanandan hyperbolic relationship (Mohammed 2016, 2017a, b, c; Mohammed and Mahmood 2018; Vipulanandan et al. 2018a, b). The Vipulanandan hyperbolic relationship to predict the maximum shear stress limit for the bentonite drilling mud and oil well cement modified with nanomaterials

(Vipulanandan and Mohammed 2015a, b, c, d, e; Mohammed 2016, 2017a, b, c).

## 1.2 Objectives

The objective of this study was to quantify the mechanical behavior of the shale rock using experimental data and more than 250 data collected from the literature. The specific objectives are as follows:

1. To qualify the statistical variation in the density, compressive strength, tensile, modulus of elasticity and fracture toughness of shale rock.
2. To investigate and quantify the correlation relation between the compression strength and tensile strength of shale rock using the Vipulanandan correlation model.
3. To investigate and quantify the correlation relation between the modulus of elasticity and fracture toughness with tensile and compressive strength of shale rock using the Vipulanandan correlation model.
4. Using nondestructive test such as the ultrasonic pulse velocity to characterize shale rock.
5. Quantify the shear failure strength for the shale rock using the Vipulanandan failure model and compare the prediction to the Mohr–Coulomb failure model.

## 2 Methods and Materials

### 2.1 Shale Rocks

Five field rock samples were used for testing. The physical and mechanical properties of the rock were tested according to ASTM Standards. These results are summarized in Table 1.

### 2.2 XRD Analysis

X-ray diffraction (XRD) was used to characterize the shale rock. The XRD patterns were obtained using the Siemens D5000 powder X-ray diffraction machine. The sample ($\approx$ 2 g) was placed in an acrylic sample holder, which was about 3 mm deep. The sample was analyzed by using parallel beam optics with CuK$\alpha$ radiation at 40 kV and 30 mA. The sample was scanned for reflections (2$\theta$) in the range 0°–90° in a step size of 0.02° and a 2 s count time per step.

### 2.3 Data Collection

This study was focused on the statically variation and correlations between density and strength properties of shale rock, based on the tested and collected data from various research studies.

This study was focused on the behavior of shale rock and the data collected from several research studies (Swapnil et al. 2004; Vipulanandan and Nam 2009; Nam and Vipulanandan 2010; Vipulanandan et al. 2015a; Mohammed and Mahmood 2018). The properties of interest were density, compressive and tensile strengths, Mode-1 fracture toughness, compressive modulus and shear strength of the shale rock. The data was collected from rocks in seven countries. The density study focused on the statistical distribution and the range of variation using 53 data on shale.

### 2.4 Strength Properties

In this study, more than 150 data of compression and tensile strengths for shale rock were collected from various research studies. The data were quantified using the Vipulanandan correlation model and compared with models used in the literature.

Table 1 Test methods and mechanical properties of shale rock

| Mechanical property | Test method | Average value |
|---|---|---|
| Density, $\gamma$ (gm/cm$^3$) | ASTM D 5195 | 2.42 |
| Compressive strength, $\sigma_c$ (MPa) | ASTM D7012 | 46 |
| Tensile strength, $\sigma_t$ (psi) | ASTM D3967 | 5.8 |
| Modulus of elasticity, E (GPa) | ASTM D3148 | 3.3 |
| Pulse velocity PV, (m/s) | ASTM D2845 | 3633 |

## 2.5 Compressive Strength Test

Unconfined compression tests were conducted according to ASTM D 7012. The cylindrical rock specimens with the diameter of 3 inches and a height of 6 inches (76 mm dia. * 152 mm height) were tested at a predetermined controlled displacement rate with a displacement rate of 1 mm/min and loading rate of 0.5 mm/min. Compression tests were performed on shale rock samples using a hydraulic compression testing machine. Commercially available 10 mm resistance strain gages were used for strain measurement. At least three samples were tested as shown in Fig. 1.

## 2.6 Split tensile Strength Tests

The split tensile tests were performed according to ASTM D 3967 Standard. For conducting the split tensile test, cylindrical specimens of size 3 inches diameter and 6 inches length were tested. The rock specimens were placed horizontally between the two bearing plates of the compression-testing machine adjusted for a machine displacement rate of 1.0 mm/min. The split tensile strength ($\sigma_t$) was obtained using the following relationship.

$$\sigma_t = \frac{2P}{\pi LD} \tag{1}$$

where P = failure load; L = thickness or length of specimen; and D = diameter of the specimen.
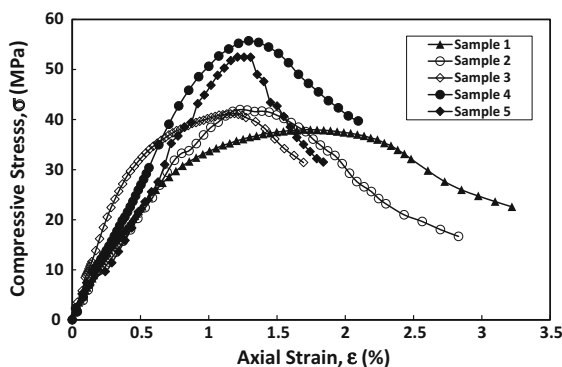


**Fig. 1** Stress–strain relationships of shale

## 2.7 Ultrasonic Pulse Velocity Test

The primary advantages of ultrasonic testing are that it produces compression and shear wave velocities, and ultrasonic values for the elastic constants of intact homogeneous isotropic rock specimens (Cannaday 1964; Swapnil et al. 2004). The propagation velocities of the compression wave, $V_p$ as follows:

$$V_P = \frac{L}{T_p}, \tag{2}$$

where, V = pulse-propagation velocity (m/s), L = pulse-travel distance (m) and T = effective pulse-travel time (measured time minus zero time correction) (s) and subscripts P denote the compression wave. Pulse velocity tests were performed on five shale samples. The frequency used to measure the pulse velocity was 150 kHz. Pulse-travel distance and time were measured to determine compression-wave velocity for shale rock. Unit weight was also calculated by measuring the weight and volume of each sample. The average compression-wave velocity of shale rock was 3233 m/s.

## 3 Modeling

### 3.1 Vipulanandan Correlation Model

Nonlinear correlation between the rock properties was investigated using the Vipulanandan correlation model for the shale rock. Based on the inspection of the data collected the following relationship was selected:

$$Y = Y_o + \frac{X}{(A + B * X)} \tag{3}$$

where, Y = Depended variable (example: tensile strength, compressive modulus, fracture toughness); $Y_o$, A and B = model parameters; X = Independent variable (example: compression strength, tensile strength, pulse velocity).

Based on the data collected the correlations were either linear or nonlinear for the material properties of interest. As shown in Fig. 2 relationship proposed in Eq. (3) can be used to represent various linear and nonlinear trends based on the values of the parameters A and B. When parameters A and B are positive, the relationship was hyperbolic. Linear relationship is
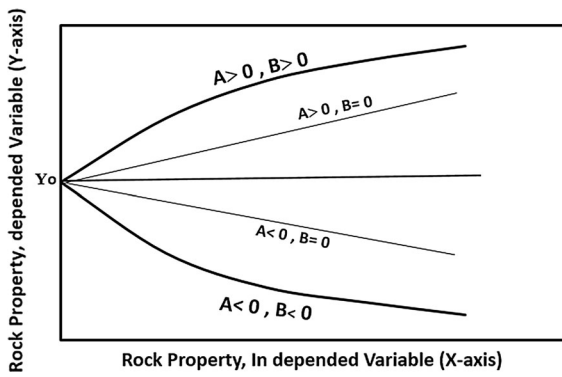
**Fig. 2** Vipulanandan model the linear and nonlinear responses of rock

represented by Eq. (3) when B = zero and A will take any value. When parameters A and B are negative, the inverse hyperbolic relationship is obtained (Vipulanandan and Mohammed 2014, 2015b). The results obtained from Eq. (3) were compared with Model-2 (Eq. 4) which has been used in the literature (Juki et al. 2013; You 2015).

$$\sigma_t = \alpha * \sqrt{\sigma_c} \qquad (4)$$

where, $\alpha$ is the correlation parameter.

## 3.2 Mohr–Coulomb Failure Model (1900)

The Mohr–Coulomb failure criterion represents the linear relationship between the shear strength of a rock and the applied normal stress on the failure plane. This relation is expressed as:

$$\tau = \tau_o + \sigma_n tan\phi \qquad (5)$$

where $\tau$ is the shear strength, $\sigma_n$ is the normal stress, $\tau_o$ is the intercept of the failure envelope with the y axis, and $\phi$ is the slope of the failure relationship. The quantity c is called the cohesion and the angle $\phi$ is called the angle of internal friction.
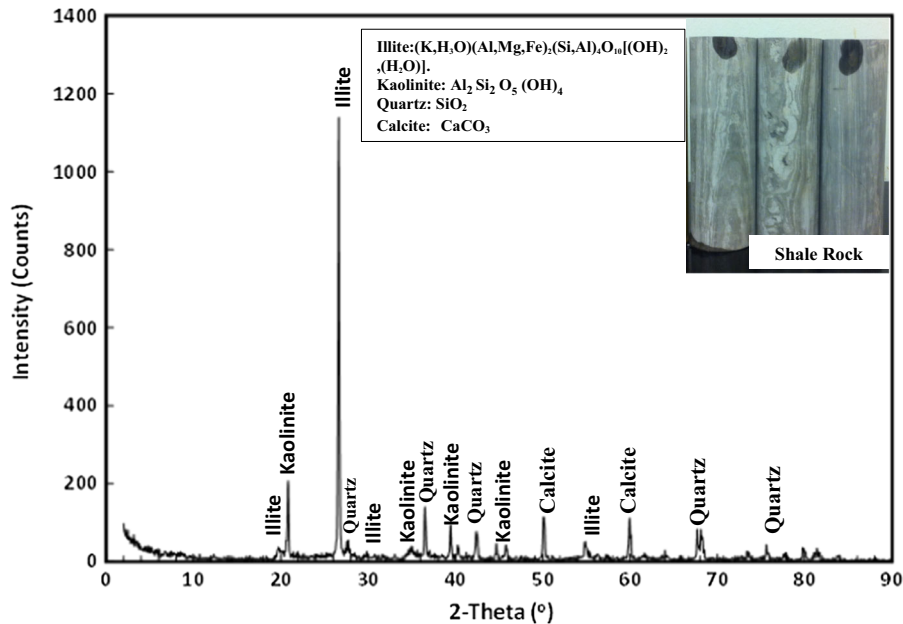
From Eq. (5)

$$\frac{d\tau}{d\sigma} = tan\varphi \qquad (6)$$

$$\frac{d^2\tau}{d\sigma^2} = 0 \qquad (7)$$

when $\sigma_n \rightarrow \infty$; $\tau = \infty$

Hence, Mohr–Coulomb failure model does not satisfy the upper limit condition for the shear strength tolerance of the materials.



**Fig. 3** XRD Pattern for shale rock

### 3.3 Vipulanandan Failure Model (2018a, b)

$$\tau = \tau_o + \frac{\sigma_n}{C + D * \sigma_n} \qquad (8)$$

$$\frac{d\tau}{d\sigma_n} = \frac{(C + D\sigma_n) - \sigma D}{(C + D\sigma_n)^2} = \frac{C}{(C + D\sigma_n)^2} > 0$$
$$\Rightarrow C > 0$$

$$\frac{d^2\tau}{d\sigma_n^2} = -2(C + D\sigma_n)^{-3} * CD = \frac{-2CD}{(C + D\sigma_n)^3} < 0,$$
$$\Rightarrow D > 0$$

when $\tau = 0 \Rightarrow$

$$0 = \tau_o + \frac{\sigma_t}{C + D * \sigma_t} \qquad (9)$$

$$\sigma_t = \frac{-\tau_o}{\frac{1}{C} + \frac{D}{C}\tau_o} \qquad (10)$$

Equation (8) is similar to Eq. (3) in characterizing the tensile strength of shale rock.

Also, when $\sigma_n \to \infty$

$$\tau_\infty = \tau_o + \frac{1}{D} \qquad (11)$$

Hence, this model (Eq. 8) has a limit on the maximum shear stress the rocks will tolerate at relatively high normal stress.

Mohr–coulomb failure relationship (linear curve fitting of data) was developed in 1900. Since then many failure relationships with quadratic and cubic terms have been developed to curve fit the test data without satisfying basic conditions. Vipulanandan failure model (not curve fitting model) is based on satisfying fundamental conditions in developing the relationship with three material parameters.

### 3.4 Comparison of Model Predictions

Both coefficient of determination ($R^2$) and the root mean square error (RMSE) for the model predictions were used in order to determine the accuracy of the model predictions as defined in Eqs. (12) and (13) were quantified.

$$R^2 = \left( \frac{\sum_i (x_i - \bar{x})(y_i - \bar{y})}{\sqrt{\sum_i (x_i - \bar{x})^2} * \sqrt{\sum_i (y_i - \bar{y})^2}} \right) \qquad (12)$$
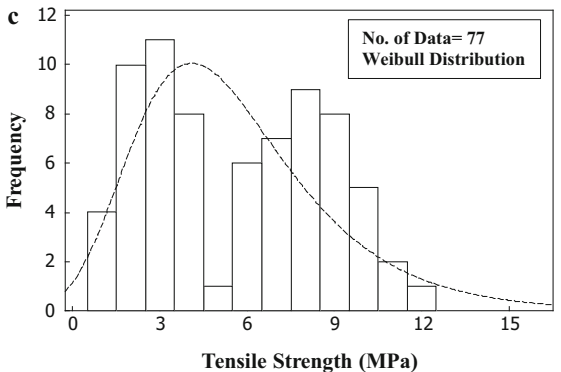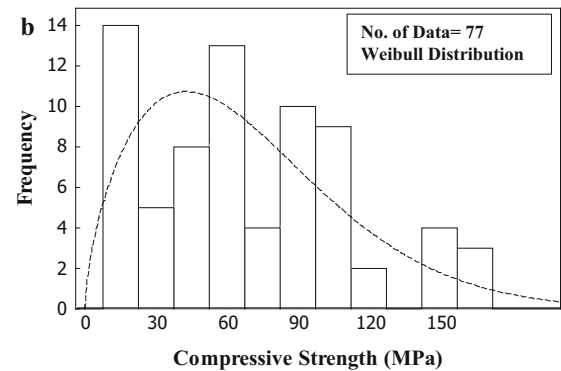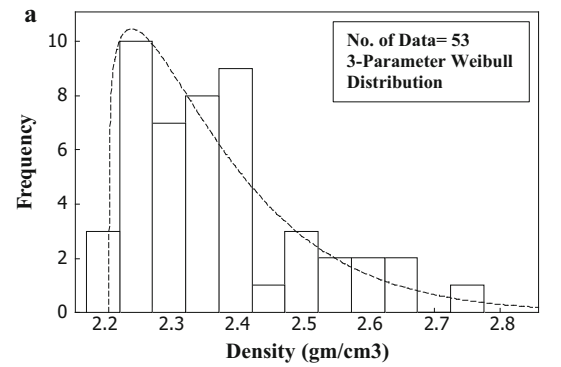


**Fig. 4** Shale rock distribution fit of **a** density, **b** compressive strength, **c** tensile strength

$$RMSE = \sqrt{\frac{\sum_{i=1}^n (y_i - x_i)^2}{N}} \qquad (13)$$

where $y_i$ = actual test value; $x_i$ = calculated value from the model; $\bar{y}$ = mean of the actual test values; $\bar{x}$ = mean of calculated values and N is the number of data points.

**Table 2** Rang of shale properties from the literature

| References | Location | Density (gm/cm³) | Tensile strength, $\sigma_t$ (MPa) | Compressive strength, $\sigma_c$ (MPa) | Shear strength (MPa) | Compression modulus, E (GPa) | Fracture toughness (MPa m$^{0.5}$) |
|---|---|---|---|---|---|---|---|
| Wang and Park (2002) | S. Korea | – | – | 28–54 | – | – | – |
| Josh et al. (2012) | Australia | – | – | – | 7–53 | – | – |
| Zhang (2002) | Sweden | – | 3.3–13 | – | – | – | 0.6–1.1 |
| Pells (2004) | Australia | – | 1.0–4 | 7.0–40 | – | 5.0–15 | – |
| Fjar et al. (2008) | USA | 2.71–2.78 | 2–10 | 5–100 | – | 5–30 | 0.027–0.041 |
| Nam and Vipulanandan (2010) | USA | 1.7–2.1 | – | – | – | 0.4–2.6 | – |
| Yesiloglu–Gultekin et al. (2013) | Turkey | – | 6.0–16 | 60–200 | – | 10–33 | – |
| Vipulanandan and Mohammed (2014) | USA | 1.9–2.7 | – | 12–45 | – | – | – |
| Mohammed and Mahmood (2018) | Iraq | 2.65–2.7 | – | 15–40 | – | – | – |
| Remark | 7 Countries | Varied between 1.70 and 2.78 gm/cm³ | Varied between 1 and 13 MPa | Varied between 5 and 200 MPa | Varied between 7 and 53 MPa | Varied between 0.4 and 33 GPa | Varied between 0.027 and 1.1 MPa m$^{0.5}$ |

## 4 Results and Analyses

### 4.1 XRD

X-Ray diffraction was used to identify and quantify the changes in shale rock with two different components such as clay mineral and no clay mineral. Clay minerals were included kaolinite ($Al_2Si_2O_5(OH)_4$)(2θ peaks at 19.75°, 20.75° and 55.30°) and illite (($K,H_{3-}O$)($Al,Mg,Fe$)$_2$($Si,Al$)$_4O_{10}$[($OH$)$_2$,($H_2O$)]) (2θ peaks at 19.75°, 20.75° and 55.30°). No clay minerals were included quartz ($SiO_2$) (2θ peaks at 43.50°) and Calcite ($CaCO_3$) as shown in Fig. 3. Similar results was reported by Butt (2012).

### 4.2 Density (γ)

Based on the total of 58 density data for shale, the data varied from 1.70 to 2.78 gm/cm³ with the standard deviation of 0.132 gm/cm³, variance 0.017 and coefficient of variation (COV) of 5.56% as summarized in Table 3. The histograms were analyzed and showed that, almost 67% of the total of γ was between 2.3 and 2.5 gm/cm³. In this study, the statistical details and the histograms were developed for each density data sets to identify the distribution. Different distribution tests for the densities for shale was performed as summarized in Table 4. Based on the Anderson–Darling statistic (AD) and P value (hypothesis testing), 3-Parameter Weibull frequency distribution for the density for shale was observed and are shown in Fig. 4a.

**Table 3** Statistical parameters of geotechnical properties of shale rocks

| Statistical parameters | Density (gm/cm$^3$) | Compressive strength, $\sigma_c$ (MPa) | Tensile Strength, $\sigma_t$ (MPa) | Compression modulus, E (GPa) | Fracture toughness (MPa m$^{0.5}$) |
|---|---|---|---|---|---|
| No. of data | 53 | 77 | 77 | 29 | 10 |
| Range | 1.70–2.78 | 5–200 | 1–13 | 0.4–33 | 0.027–1.1 |
| Mean ($\mu$) | 2.35 | 57 | 5.96 | 15.30 | 0.76 |
| Std. deviation ($\sigma$) | 0.132 | 43.17 | 3.1 | 1.18 | 0.19 |
| Variance ($\sigma^2$) | 0.017 | 1863 | 9.48 | 1.38 | 0.036 |
| COV (%) | 5.56 | 62.43 | 55.13 | 7.68 | 23.86 |

**Table 4** Distribution identification of shale rocks

| Properties | Distribution fit | $P$ value | AD |
|---|---|---|---|
| Density (gm/cm$^3$) | Largest extreme value | 0.132 | 0.585 |
| | 2-Parameter exponential | 0.186 | 0.768 |
| | 3-Parameter Weibull | 0.453 | 0.366 |
| Compressive strength, $\sigma_c$ (MPa) | Normal | 0.009 | 1.046 |
| | Gama | 0.010 | 1.063 |
| | Weibull | 0.036 | 0.806 |
| | Largest extreme value | 0.022 | 0.884 |
| Tensile strength, $\sigma_t$ (MPa) | 2-Parameter exponential | < 0.010 | 2.733 |
| | Weibull | < 0.010 | 1.775 |
| | Smallest extreme value | < 0.010 | 1.852 |
| | Largest extreme value | < 0.010 | 1.975 |

### 4.3 Strength Properties
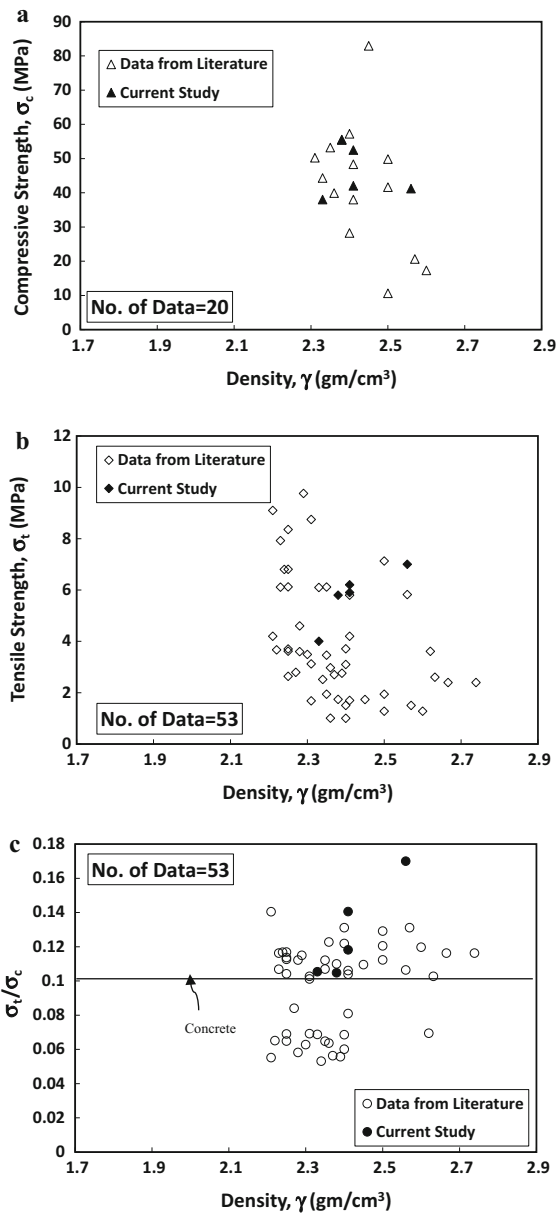
#### 4.3.1 Compressive Strength ($\sigma_c$)

Based on the 5 experimental data and 72 data of the shale rock collected from literature (Table 2), the compressive strength data for shale rock varied from 5 to 200 MPa with a mean of 57 MPa, the standard deviation of 43.17 MPa and coefficient of variation (COV) of 62.43% as summarized in Table 3. The histograms were also analyzed and showed that, more than 76% of the total of $\sigma_c$ was between 30 and 90 MPa. Different distribution tests for the compressive strength for shale was performed as summarized in Table 4. Based on the Anderson–Darling statistic (AD) and $P$ value, Weibull frequency distribution for the density for shale was observed and are shown in Fig. 4b.

#### 4.3.2 Tensile Strength ($\sigma_t$)

Based on the 5 experimental data and 72 of the shale rock collected from literature (Table 2), the tensile strength data for shale rock was varied from 1 to 13 MPa with a mean of 5.96 MPa, the standard deviation of 3.1 MPa and coefficient of variation (COV) of 55.13% as summarized in Table 3. The histograms were also analyzed and showed that, more than 25% of the total of $\sigma_t$ was between 4 and 8 MPa. In addition, different distribution tests for the tensile strength for shale was performed as summarized in Table 4. Based on the Anderson–Darling statistic (AD) and $P$ value, similar to compressive strength, the Weibull frequency distribution for the tensile strength of the shale was observed and are shown in Fig. 4c.

There were no direct correlations between the compression strength, tensile strength and density ($\gamma$) of the shale rock as shown in Fig. 5.

**a**



**b**



**c**



**Fig. 5** Variation of strengths with density for shale **a** compression, **b** tensile and **c** tensile/compression ratio

### 4.4 Relationship Between Compressive Strength (σ$_c$) and Tensile Strength (σ$_t$)

Based on the total of 30 shale of tested and collected data from various research studies. With increasing of $\sigma_c$ of rocks, the $\sigma_t$ nonlinearly also increased as shown in Fig. 6. The change in the $\sigma_c$ with $\sigma_t$ of rocks was represented using Vipulanandan correlation model
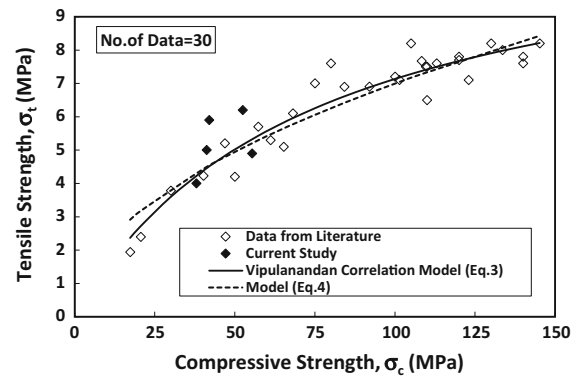


**Fig. 6** Variation of tensile strength with compressive strength for shale

relationship (Eq. 3) and the model parameters A, B, coefficient of determination ($R^2$) and root mean square error (RMSE) were 5.9, 0.081, 0.93 and 0.50 MPa respectively as summarized in Table 5. The tensile strength to compressive strength ratio of the shale rocks varied from 0.05 to 0.18 compared to 0.1 for concrete and more than 50% of the $\frac{\sigma_t}{\sigma_c}$ data were more than 0.1 as shown in Fig. 5c.

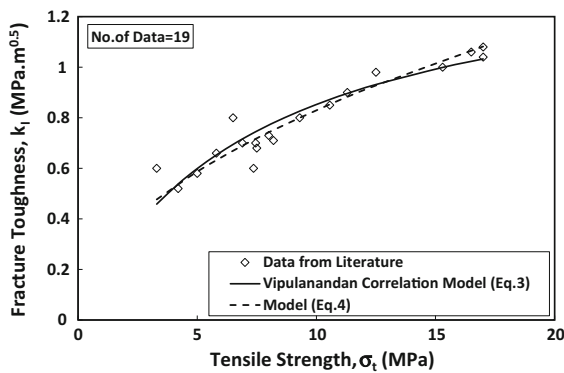### 4.5 Relationship Between Fracture Toughness (K$_I$) and Tensile Strength (σ$_t$)

Based on the total of 19 shale data were collected from various research studies. With the increase in $\sigma_t$, the K$_I$ increased nonlinearly as shown in Fig. 7. The change in the $\sigma_t$ of rocks, the fracture toughness (K$_I$) of rock was represented using Vipulanandan correlation model relationship (Eq. 3) and the model parameters A, B, coefficient of determination ($R^2$) and root mean square error (RMSE) were 4.96, 0.68, 0.82 and 0.08 MPa m$^{0.5}$ respectively as summarized in Table 5.

### 4.6 Relationship Between Compressive Strength (σ$_c$) and Pulse Velocity (PV)

Based on the five experimental data and total of 50 data were collected from various research studies. With increasing of $\sigma_c$ the PV nonlinearly increased as shown in Fig. 8a. The change in the $\sigma_c$ of shale rocks, the pulse velocity (PV) of rock was represented using Vipulanandan correlation model relationship (Eq. 3) and the model parameters A, B, coefficient of determination ($R^2$) and root mean square error (RMSE)

**Table 5** Model parameters for tensile, compression modulus, fracture toughness, compression strength and pulse velocity relationships of shale

| Depended variable (Y-axis) | In depended variable (X-axis) | Model (Eq. 4) | | | Vipulanandan correlation model (Eq. 3) | | | | No. of data | Fig. no. |
|---|---|---|---|---|---|---|---|---|---|---|
| | | $\alpha$ | RMSE | $R^2$ | A | B | RMSE | $R^2$ | | |
| Tensile strength, $\sigma_t$ (MPa) | Compressive strength, $\sigma_c$ (MPa) | 0.70 | 0.48 | 0.93 | 5.90 | 0.081 | 0.50 | 0.93 | 30 | 6 |
| Fracture toughness (MPa m$^{0.5}$) | Tensile strength, $\sigma_t$ (MPa) | 0.26 | 0.07 | 0.84 | 4.96 | 0.68 | 0.08 | 0.82 | 19 | 7 |
| Compressive strength, $\sigma_c$ (MPa) | Pulse velocity PV, (m/s) | 1.08 | 14.8 | 0.73 | 30.6 | 0.007 | 2.81 | 0.85 | 50 | 8 (a) |
| Tensile strength, $\sigma_t$ (MPa) | Pulse velocity PV, (m/s) | 0.16 | 1.47 | 0.70 | 343 | 0.01 | 1.03 | 0.86 | 16 | 8 (b) |
| Compression modulus, E (GPa) | Pulse velocity PV, (m/s) | 0.27 | 4.17 | 0.60 | 219.2 | 0.0 | 1.30 | 0.87 | 21 | 8 (c) |



**Fig. 7** Variation of fracture toughness with tensile strength for shale

were 30.6, 0.007, 0.85 and 2.81 MPa respectively, as summarized in Table 5.

### 4.7 Relationship Between Tensile Strength ($\sigma_t$) and Pulse Velocity (PV)

Based on the five experimental data and total of 16 data were collected from various research studies. With increasing of $\sigma_t$ the PV also nonlinearly increased as shown in Fig. 8b. The change in the $\sigma_t$ of shale rocks, the pulse velocity (PV) of rock was represented using Vipulanandan correlation model relationship (Eq. 3) and the model parameters A, B, coefficient of determination ($R^2$) and root mean square error (RMSE) were 343, 0.01, 0.86 and 1.03 MPa respectively, as summarized in Table 5.

### 4.8 Relationship Between Modulus of Elasticity (E) and Pulse Velocity (PV)

Based on the five experimental data and total of 21 shale data were collected from various research studies. With increasing of PV, the E nonlinearly increased as shown in Fig. 8c. The change in the modulus of elasticity (E) of shale rocks, the pulse velocity (PV) of shale rock was represented using Vipulanandan correlation model relationship (Eq. 3) and the model parameters A, B, coefficient of determination ($R^2$) and root mean square error (RMSE) were 219.2, 0, 0.87 and 1.3 MPa respectively, as summarized in Table 5.

### 4.9 Shear Stress-Normal Stress Failure Models

Shear stress-normal stress relationships was predicted using the Vipulanandan failure model and compared with the Mohr–Coulomb failure model as shown in Fig. 9.

### 4.10 Mohr–Coulomb Failure Model

The shear stress behavior of the 29 data of the shale collected from the literature was modeled using the Mohr–Coulomb failure (Eq. 5) as shown in Fig. 10. The coefficient of determination ($R^2$) and root mean square of error (RMSE) were 0.95 and 5.2 MPa respectively as summarized in Table 6. The yield stress ($\tau_o$), angle of internal friction ($\phi$) and tensile
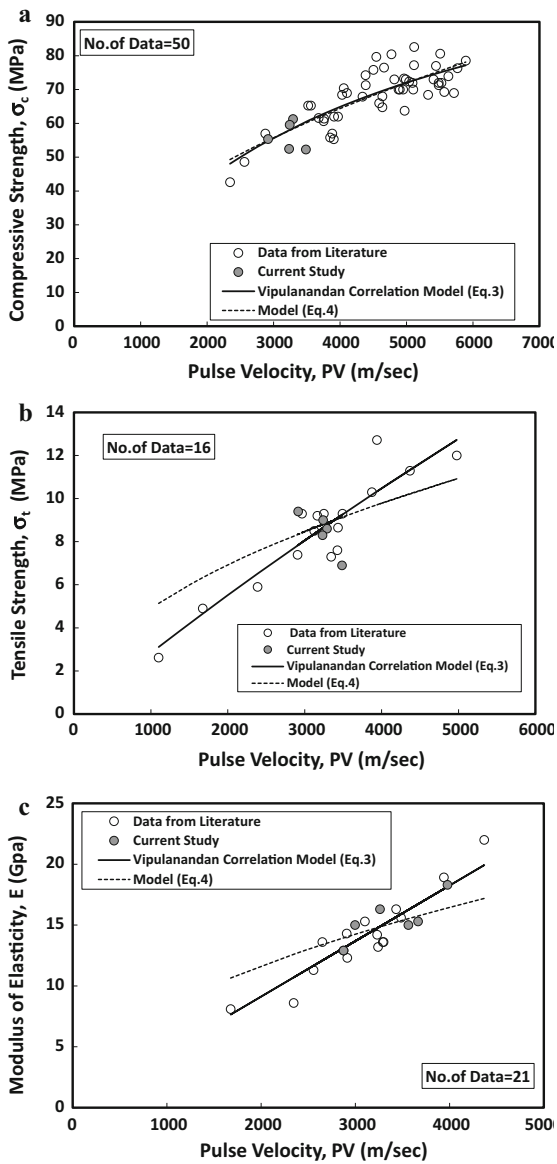
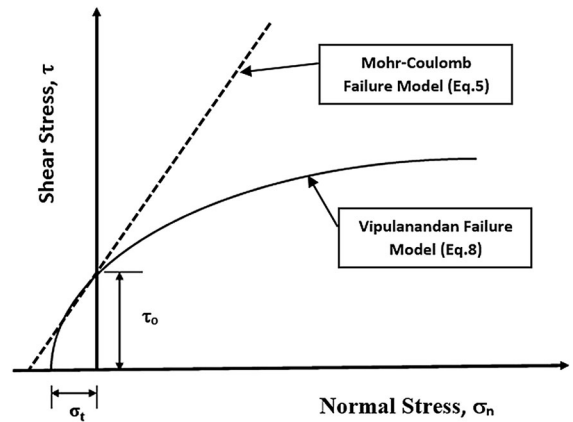**Fig. 8** Variation of **a** compressive strength, **b** tensile strength and **c** modulus of elasticity with pulse velocity for shale rock
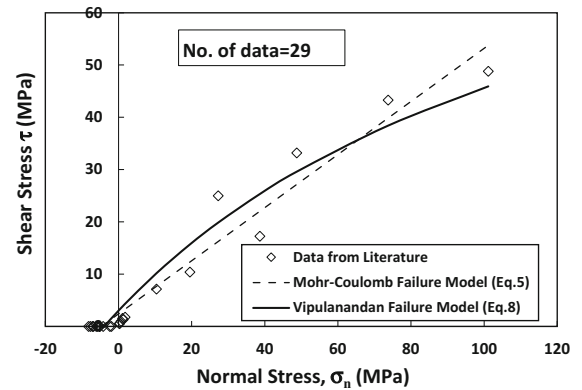


**Fig. 9** Vipulanandan failure mode compared to Mohr–Coulomb model



**Fig. 10** Variation of shear and normal stress of shale

and 2.6 MPa respectively as summarized in Table 5. The yield stress ($\tau_o$) and tensile strength ($\sigma_t$) of the shale was 3 and 3.9 MPa respectively as summarized in Table 6. The model parameter C and D for shale were 1.34 and 0.01 MPa$^{-1}$ respectively as summarized in Table 6.

### 4.12 Maximum Shear Stress ($\tau_{max.}$)

Based on Eq. (11), the Vipulanandan failure model has a limit on the maximum shear stress the rocks will produce at relatively at very large normal stress. The $\tau_{max}$ for shale was 103 MPa as summarized in Table 6.

The coefficient of determination ($R^2$) and root mean square error are methods used to quantify the errors. Visual observation (appearance) doesn't quantify the error. The Model-3 shows better correlations than

strength ($\sigma_t$) of the shale rock were 2.5 MPa, 25° and 6.5 MPa respectively as summarized in Table 6.

### 4.11 Vipulanandan Failure Model

The shear stress behavior of the 29 data of the shale collected from the literature using the Vipulanandan failure model (Eq. 8). The coefficient of determination ($R^2$) and root mean square of error (RMSE) were 0.95

**Table 6** Model parameters for shear and normal stresses relationship of shale rock

| Mohr–Coulomb model (Eq. 5) | | | | | Vipulanandan failure model (Eq. 8) | | | | | | | No. of data | Fig. no. |
|---|---|---|---|---|---|---|---|---|---|---|---|---|---|
| $\tau_o$ (MPa) | $\phi$ (°) | $\sigma_t$ (MPa) | RMSE (MPa) | $R^2$ | $\tau_o$ (MPa) | $\sigma_t$ (MPa) | C | D | $\tau_{max.}$ (MPa) (Eq. 11) | RMSE (MPa) | $R^2$ | | |
| 2.5 | 25 | 6.5 | 5.2 | 0.95 | 3 | 3.9 | 1.34 | 0.01 | 103 | 2.6 | 0.95 | 29 | 10 |

Model 4 used in the literature based on the $R^2$ and RMSE (Table 5).

The nonlinear Vipulanandan failure model is a generalized failure model, developed based on fundamental criteria. When material parameter B is zero it, represent the Mohr–Coulomb model. Therefore, Vipulanandan model will also represent Mohr–coulomb model. Using the data in the literature, the Vipulanandan failure model was compared to the Mohr–coulomb model and the results are summarized in Table 6. In addition, the Vipulanandan failure model (Eq. 11) has a limit on the maximum shear stress the rocks will tolerate at relatively high normal stress. But the linear Mohr–Coulomb failure model (Eq. 5) does not satisfy the upper limit condition for the shear strength tolerance of the materials.

## 5 Conclusions

The focus of this study was to characterize the rocks based on the density and strength properties. Based on the collected data from the literature and analytical model, the following conclusions were advanced:

1. Based on the statistical analysis the mean density of the shale was 2.35 gm/cm$^3$. The compressive strength ($\sigma_c$) of the shale varied between 5 and 200 MPa. The maximum density of the shale was 2.78 gm/cm$^3$.
2. The variation of strength properties of the rocks showed good correlation between the compressive strength with tensile strength and modulus of elasticity of the rocks.
3. The variation of tensile strength of the rocks showed good correlation between the tensile strength and fracture toughness of the shale rock.
4. There were no direct correlations between the compression strength, tensile strength and density ($\gamma$) of the shale rock. The tensile strength to

compressive strength ratio of the three rocks varied from 0.05 to 0.18 compared to 0.1 for concrete.
5. The Vipulanandan correlation model was effective in predicting the relationship between tensile strength and compressive strength of the shale rock.
6. The Vipulanandan failure criterion has been used to not only better quantify the shear stress but also maximum shear stress ($\tau_{max.}$) of the shale rock, which was 103 MPa.

## References

Butt AS (2012) Shale characterization using X-ray diffraction. Doctoral dissertation, thesis, Master of Engineering, Universitas Dalhousie, Halifax, Nova Scotia

Cannaday FX (1964) Modulus of elasticity of a rock determined by four different methods, Report of Investigations U.S. Bureau of Mines 6522

Fjar E, Holt RM, Raaen AM, Risnes R, Horsrud P (2008) Petroleum related rock mechanics, vol 53. Elsevier, New York

Josh M, Esteban L, Delle Piane C, Sarout J, Dewhurst DN, Clennell MB (2012) Laboratory characterization of shale properties. J Pet Sci Eng 88:107–124

Juki MI, Awang M, Annas MMK, Boon KH, Othman N, Roslan MA, Khalid FS (2013) Relationship between compressive, splitting tensile and flexural strength of concrete containing granulated waste Polyethylene Terephthalate (PET) bottles as fine aggregate. In: Advanced materials research, vol 795. Trans Tech Publications, pp 356–359. https://doi.org/10.4028/www.scientific.net/AMR.795.356

Karakus M, Kumral M, Kilic O (2005) Predicting elastic properties of intact rocks from index tests using multiple regression modelling. Int J Rock Mech Min Sci 42(2):323–330

Ludovico-Marques M, Chastre C, Vasconcelos G (2012) Modelling the compressive mechanical behaviour of granite

and sandstone historical building stones. Constr Build Mater 28(1):372–381

Meng Z, Pan J (2007) Correlation between petrographic characteristics and failure duration in clastic rocks. Eng Geol 89(3):258–265

Mohammed AS (2016) Effect of temperature on the rheological properties with shear stress limit of iron oxide nanoparticle modified bentonite-drilling muds. Egypt J Pet 26:791–802

Mohammed AS (2017a) Electrical resistivity and rheological properties of sensing bentonite-drilling muds modified with lightweight polymer. Egypt J Pet 27:55–63

Mohammed A (2017b) Vipulanandan model for the rheological properties with ultimate shear stress of oil well cement modified with nanoclay. Egypt J Pet. https://doi.org/10.1016/j.ejpe.2017.05.007

Mohammed AS (2017c) Property correlations and statistical variations in the geotechnical properties of (CH) clay soils. Geotech Geol Eng 36(1):267–281

Mohammed A, Mahmood W (2018) Vipulanandan failure models to predict the tensile strength, compressive modulus, fracture toughness and ultimate shear strength of calcium rocks. Int J Geotech Eng. https://doi.org/10.1080/19386362.2018.1468663

Mohammed AS, Vipulanandan C (2014) Compressive and tensile behavior of polymer treated sulfate contaminated CL soil. Geotech Geol Eng 32(1):71–83

Mohammed A, Vipulanandan C (2015) Testing and modeling the short-term behavior of Lime and Fly Ash treated sulfate contaminated CL soil. Geotech Geol Eng 33(4):1099–1114

Moos D, Peska P, Finkbeiner T, Zoback M (2003) Comprehensive wellbore stability analysis utilizing quantitative risk assessment. J Petrol Sci Eng 38(3):97–109

Nam MS, Vipulanandan C (2010) Relationship between texas cone penetrometer tests and axial resistances of drilled shafts socketed in Clay Shale and limestone. J Geotech Geoenviron Eng 136(8):1161–1165

Omar M (2017) Empirical correlations for predicting strength properties of rocks—United Arab Emirates. Int J Geotech Eng 11(3):248–261

Ozturk CA, Nasuf E (2013) Strength classification of rock material based on textural properties. Tunn Undergr Space Technol 37:45–54

Pells PJN (2004) Substance and mass properties for the design of engineering structures in the Hawkesbury sandstone. Aust Geomech 39(3):1–21

Rajabzadeh MA, Moosavinasab Z, Rakhshandehroo G (2012) Effects of rock classes and porosity on the relation between uniaxial compressive strength and some rock properties for carbonate rocks. Rock Mech Rock Eng 45(1):113–122

Sabatakakis N, Koukis G, Tsiambaos G, Papanakli S (2008) Index properties and strength variation controlled by microstructure for sedimentary rocks. Eng Geol 97(1):80–90

Sandrea R (2012) Evaluating production potential of mature US oil, gas shale plays. Oil Gas J 110(12):58

Schmidt RA (1976) Fracture-toughness testing of limestone. Exp Mech 16(5):161–167

Swapnil K, Kim MG, Vipulanandan C (2004) Nondestructive properties of Clayshale and Limestone in Dallas, Texas. In: Gulf rocks 2004, the 6th North America rock mechanics

symposium (NARMS). American Rock Mechanics Association

Usluogullari OF, Vipulanandan C (2011) Stress–strain behavior and California bearing ratio of artificially cemented sand. J Test Eval 39(4):1–9

Vipulanandan C, Nam E (2009) Drilled shaft socketed in uncemented clay shale. Proceedings, foundation congress 2009. Contemporary topics in deep foundations, ASCE, GSP 185, pp 151–158

Vipulanandan C, Mohammed AS (2014) Hyperbolic rheological model with shear stress limit for acrylamide polymer modified bentonite-drilling muds. J Petrol Sci Eng 122:38–47

Vipulanandan C, Mohammed AS (2015a) Characterizing the hydraulic fracturing fluid modified with nano silica proppant. AADE-15-NTCE-38, CD Proceeding, San Antonio, Texas, April 2015

Vipulanandan C, Mohammed A (2015b) Effect of nanoclay on the electrical resistivity and rheological properties of smart and sensing bentonite drilling muds. J Petrol Sci Eng 130:86–95

Vipulanandan C, Mohammed A (2015c) XRD and TGA, swelling and compacted properties of polymer treated sulfate contaminated CL soil. J Test Eval 44(6):2270–2284

Vipulanandan C, Mohammed A (2015d) Smart cement modified with iron oxide nanoparticles to enhance the piezoresistive behavior and compressive strength for oil well applications. Smart Mater Struct 24(12):125020

Vipulanandan C, Mohammed A (2015e) Smart cement rheological and piezoresistive behavior for oil well applications. J Petrol Sci Eng 135:50–58

Vipulanandan C, Mohammed A (2017a) Rheological properties of piezoresistive smart cement slurry modified with iron-oxide nanoparticles for oil-well applications. J Test Eval 45(6):2050–2060

Vipulanandan C, Mohammed A (2017b) Smart cement compressive piezoresistive, stress–strain, and strength behavior with nanosilica modification. J Test Eval. https://doi.org/10.1520/JTE20170105

Vipulanandan C, Mohammed A (2018) New Vipulanandan failure model and property correlations for sandstone, shale and limestone rocks. In: IFCEE 2018, pp 365–376

Vipulanandan C, Mohammed A (2018) New Vipulanandan failure model and property correlations for sandstone, shale and limestone rocks. IFCEE 2018:365–376

Vipulanandan C, Krishnamoorti R, Mohammed A, Boncan V, Narvaez G, Head B, Pappas JM (2015) Iron nanoparticle modified smart cement for real time monitoring of ultra deepwater oil well cementing applications. In: Offshore technology conference. Offshore technology conference

Vipulanandan C, Mohammed A, Samuel RG (2017) Smart bentonite drilling Muds modified with iron oxide nanoparticles and characterized based on the electrical resistivity and rheological properties with varying magnetic field Strengths and temperatures. OTC-MS-270626

Vipulanandan C, Mohammed A, Ganpatye AS (2018a) Smart cement performance enhancement with nano $Al_2O_3$ for real time monitoring applications using Vipulanandan models. In: Offshore technology conference. Offshore technology conference

Vipulanandan C, Mohammed A, Samuel RG (2018b) Fluid loss control in smart bentonite drilling mud modified with nanoclay and quantified with Vipulanandan fluid loss model. In: Offshore technology conference. Offshore technology conference

Wang JA, Park HD (2002) Fluid permeability of sedimentary rocks in a complete stress–strain process. Eng Geol 63(3):291–300

Yesiloglu-Gultekin N, Gokceoglu C, Sezer EA (2013) Prediction of uniaxial compressive strength of granitic rocks by various nonlinear tools and comparison of their performances. Int J Rock Mech Min Sci 62:113–122

You M (2015) Strength criterion for rocks under compressive-tensile stresses and its application. J Rock Mech Geotech Eng 7(4):434–439

Zhang ZX (2002) An empirical relation between mode I fracture toughness and the tensile strength of rock. Int J Rock Mech Min Sci 39(3):401–406

Zoback MD, Barton CA, Brudy M, Castillo DA, Finkbeiner T, Grollimund BR, Wiprut DJ (2003) Determination of stress orientation and magnitude in deep wells. Int J Rock Mech Min Sci 40(7):1049–1076